iScience

CellPress
OPEN ACCESS

Article

Caffeine-induced release of small molecules from DNA nanostructures

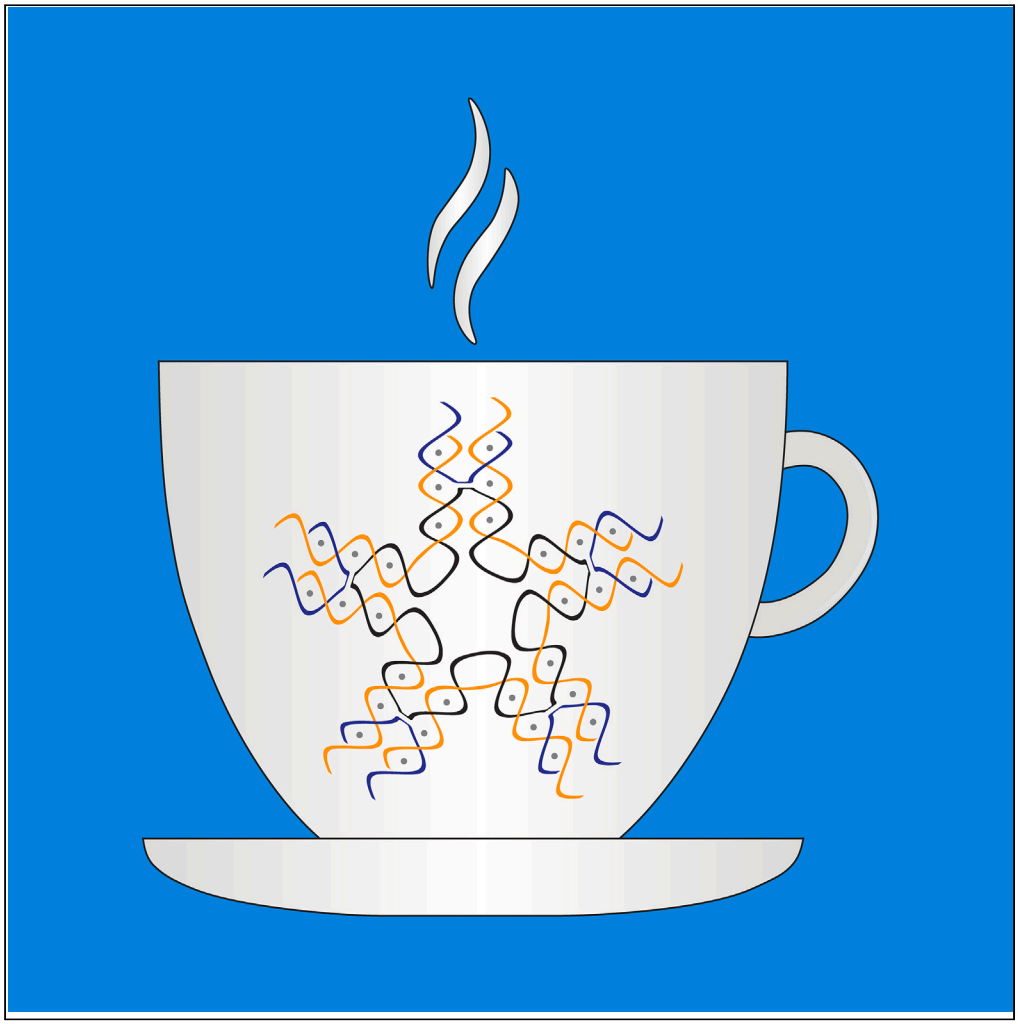

Bharath Raj Madhanagopal, Sabrina Chen, Ché-Doni Platt, Arun Richard Chandrasekaran

arun@albany.edu

Highlights

Caffeine causes deintercalation of ethidium bromide from DNA nanostructures

Duplex, four-way junction, double crossover, and tensegrity triangle motif were tested

Caffeine impedes the binding of ethidium bromide in all four structures to the same extent

Nanostructure complexity slightly affects deintercalation profiles

Madhanagopal et al., iScience *26*, 106564
May 19, 2023
https://doi.org/10.1016/j.isci.2023.106564

iScience

CellPress
OPEN ACCESS

Article

Caffeine-induced release of small molecules from DNA nanostructures

Bharath Raj Madhanagopal,[1] Sabrina Chen,[1] Ché-Doni Platt,[1] and Arun Richard Chandrasekaran[1,2,*]

SUMMARY

Several planar aromatic molecules are known to intercalate between base pairs of double-stranded DNA. This mode of interaction has been used to stain DNA as well as to load drug molecules onto DNA-based nanostructures. Some small molecules are also known to induce deintercalation in double-stranded DNA, one such molecule being caffeine. Here, we compared the ability of caffeine to cause deintercalation of ethidium bromide, a representative DNA intercalator, from duplex DNA and three DNA motifs of increasing structural complexity (four-way junction, double crossover motif, and DNA tensegrity triangle). We found that caffeine impedes the binding of ethidium bromide in all these structures to the same extent, with some differences in deintercalation profiles. Our results can be useful in the design of DNA nanocarriers for intercalating drugs, where drug release can be chemically stimulated by other small molecules.

INTRODUCTION

Interaction with small molecules is a necessary component of several applications of DNA nanostructures. One mode of interaction of such small molecules is by intercalation between the base pairs of double-stranded DNA. In some cases, these small molecules show enhanced fluorescence emission upon intercalation.[1] In DNA nanotechnology, such fluorescent intercalating small molecules are used in gel-based readout of diagnostic DNA nanoswitches,[2] fluorescence microscopy imaging of DNA nanostructures,[3] to create high-density DNA nanotags for bioimaging[4] and to chemically functionalize one-dimensional DNA arrays.[5] This mode of interaction is also convenient for loading drug molecules that are known to bind DNA by intercalation.[6–8] DNA nanostructures are ideally suited as carriers of DNA intercalators to achieve targeted delivery with high drug loading efficiency and cell penetrability.[9,10] Understanding the interaction of other small molecules with DNA-bound drugs would add to the advantageous features of DNA nanotechnology-based drug delivery, such as in the release of intercalating drugs from DNA nanocarriers by small molecules.

Recent work by other groups have investigated the interaction of intercalating small molecules with DNA nanostructures,[11–13] but to our knowledge no reports are available on small molecule-triggered deintercalation from DNA nanostructures. Here, we studied the ability of caffeine (1,3,7-trimethylxanthine) to deintercalate ethidium bromide (EBr), a representative intercalator, from DNA nanostructures (Figure 1A). Caffeine, an alkaloid present in various beverages, is a stimulant of the central nervous system[14] and has been shown to interact with DNA and inhibit DNA repair.[15,16] Caffeine prevents the binding of intercalating small molecules to DNA by forming hetero-association complexes with the molecules.[17] For example, caffeine has been shown to displace fluorescent intercalators such as EBr, propidium iodide, and 7-aminoactinomycin D from genomic DNA previously stained with these dyes.[18] Caffeine also interacts with small molecule drugs (e.g.: doxorubicin and ellipticine) and reduces their pharmacological activity.[19] In the case of EBr, caffeine disrupts DNA-EBr complex formation through hetero-association with the dye at low DNA concentrations, while at higher concentrations of DNA, it binds to DNA and competes with the dye.[20] Although the ability of caffeine to cause dissociation of intercalators from linear double-stranded DNA is well known, the same has not been demonstrated for DNA nanostructures. Our study on the interaction of DNA nanostructures with small molecules can inform and improve the design principles used to develop DNA-based nanocarriers for loading and release of DNA-intercalating small molecules.

[1]The RNA Institute, University at Albany, State University of New York, Albany, NY 12222, USA

[2]Lead contact

*Correspondence: arun@albany.edu

https://doi.org/10.1016/j.isci.2023.106564

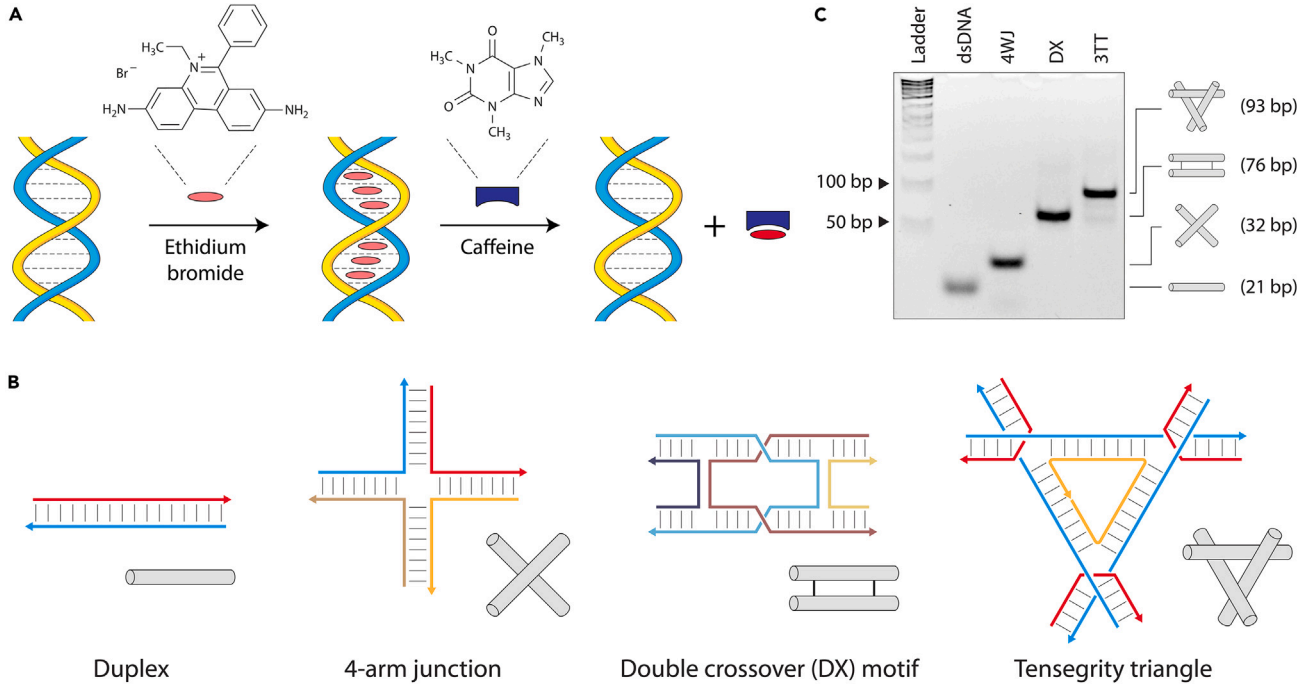

Figure 1. Design and overview

(A) Schematic showing the intercalation of ethidium bromide (EBr) to DNA and deintercalation triggered by caffeine.

(B) Model DNA nanostructures used in this study: a duplex, a four-way junction (4WJ), a double crossover (DX) motif, and a 3-helical-turn per edge tensegrity triangle (3TT) motif.

(C) Non-denaturing PAGE showing assembly of the structures. See Table S1 for full sequences and Figure S1 for designs of the structures with sequences.

RESULTS AND DISCUSSION

As model structures for this study, we chose a four-way junction (4WJ), a double crossover (DX) motif, and a 3-helical-turn per edge tensegrity triangle (3TT) motif with one, two, and three crossovers in the structures, respectively (Figures 1B and S1). Four-way junctions[21] are an integral part of several DNA nanostructures that contain strand crossovers including DNA origami, and the DX motif[22] has been used in the construction of 2D lattices and higher-order tubular structures.[23,24] The tensegrity triangle motif, originally designed to create 2D DNA arrays,[25] is the basic unit of rationally designed 3D DNA crystals.[26,27] As a control structure, we used a 21 base pair duplex. Compared to simple DNA duplexes, these structures have increasing numbers of strand crossovers, a common design parameter in DNA nanostructures, representing increasing topological complexity. We assembled the DNA structures by mixing stoichiometric ratios of component DNA strands in tris-acetate-EDTA (1× TAE-Mg^{2+}) buffer followed by a thermal annealing step (see method details). We characterized the assembly of the structures using non-denaturing PAGE, a method now well established by our group[27–30] and others[22,25] to validate the assembly of such DNA motifs (Figure 1C).

Next, we studied the interaction between EBr and DNA using fluorescence spectroscopy. Since the fluorescence emission of EBr increases upon its intercalation into double stranded DNA,[31] we obtained the emission spectra and monitored the changes in the fluorescence intensity of EBr at 600 nm (corresponding to the emission peak of EBr) in the presence of DNA. To compare the fluorescence emission changes in DNA structures of different lengths and molecular weights, we express the concentration of DNA as base pairs (BPs). We incubated different concentrations of the DNA nanostructures (10 μM BPs to 40 μM BPs) with 20–80 μM EBr and obtained the fluorescence spectra from wavelengths 540–720 nm (Figure S2). We calculated the fold change in the fluorescence emission signal at 600 nm for different DNA concentrations of all the structures (Figures 2 and S3). We observed the highest fold change in signal at 40 μM BPs and 20 μM EBr and chose this condition for further experiments. At higher EBr concentrations, the fluorescence fold change decreased suggesting an increase in the amount of unbound EBr molecules in the solution (Figure S3). The enhancement of EBr fluorescence in duplex DNA was slightly higher than that in the

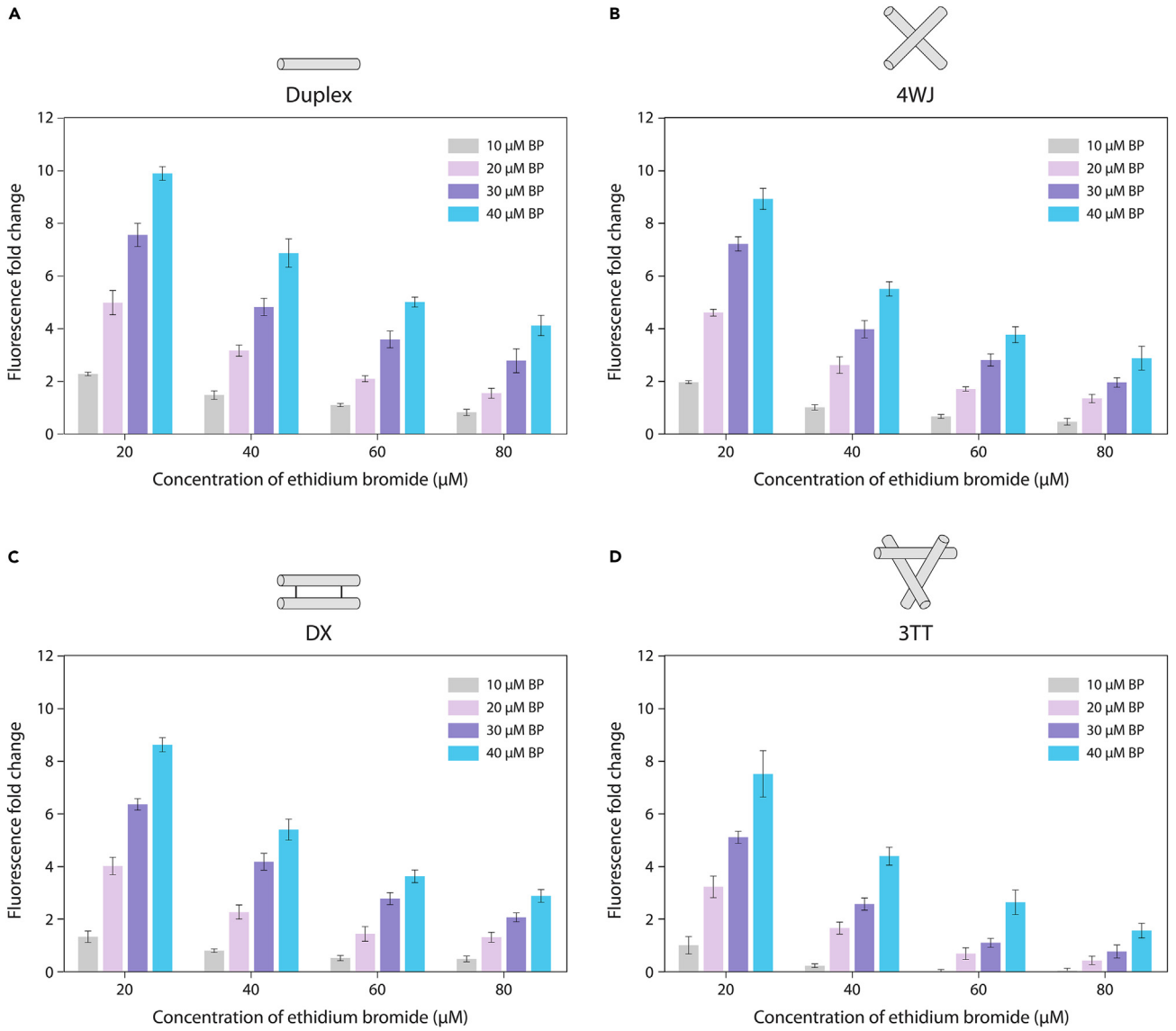

Figure 2. Binding of ethidium bromide to DNA nanostructures

Fold change in fluorescence emission at 600 nm of EBr (20–80 μM) upon intercalation into different concentrations of (A) duplex DNA, (B) 4WJ, (C) DX motif, and (D) 3TT. DNA concentrations are indicated as base pairs (BP). Data represent mean and error propagated from standard deviations of triplicate experiments. See Figure S2 for representative fluorescence spectra and Figure S3 for raw fluorescence data.

DNA nanostructures, possibly due to the presence of crossovers that occlude intercalation of EBr. Moreover, EBr intercalation is known to unwind the duplex.[32] Such changes in the helicity could be more easily accommodated in simple duplexes with free termini compared to the double helical regions restricted by one or more crossovers in the DNA nanostructures.

Next, we studied how caffeine affects the ability of EBr to intercalate different DNA nanostructures. We mixed EBr (20 μM) with different concentrations of caffeine (0–25 mM), followed by the addition of DNA nanostructures or duplex DNA (40 μM BP). We incubated the mixtures at 20°C for 30 min and monitored the change in fluorescence emission at 600 nm (Figure 3). To compare the effect of caffeine on the interaction of EBr to the different structures, we normalized the fluorescence fold change and calculated the intercalation index, which is the ratio of the observed fluorescence fold change in [caffeine-EBr-DNA] solutions and the fold change in [EBr-DNA] solution. For all the structures, we observed an exponential

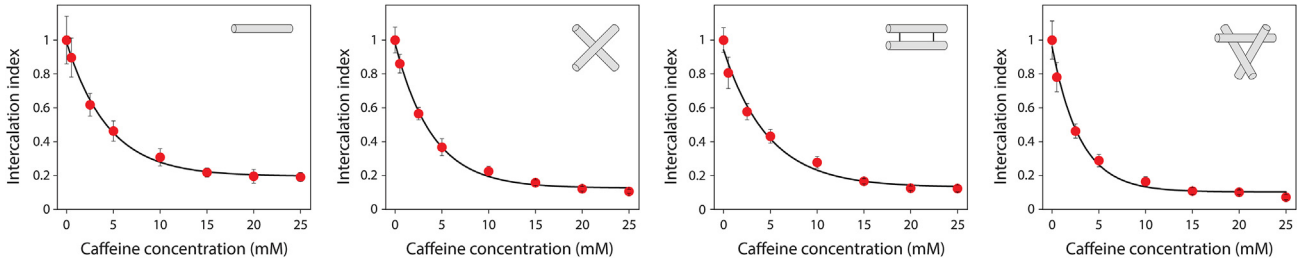

Figure 3. Caffeine inhibits binding of ethidium bromide to DNA nanostructures

Calculated intercalation indices showing reduced binding of EBr (20 μM) to DNA nanostructures (40 μM BP) with increasing concentrations of caffeine. Values are normalized to intensities obtained in the absence of caffeine. Data represent mean and error propagated from standard deviations of triplicate experiments. See Figure S4 for a plot containing data from all four structures overlapped.

decrease in the intercalation index with increase in caffeine concentration indicating that caffeine impedes the intercalation of EBr into DNA nanostructures at a level similar to that in duplex DNA (Figures 3 and S4).

After confirming that caffeine inhibits EBr binding to DNA, we tested whether caffeine can deintercalate EBr already bound to DNA nanostructures. We prepared DNA-EBr complexes at the same ratio as before but at a higher concentration (60 μM EBr and 120 μM BP for DNA) and added 50 mM caffeine to the solution and monitored the changes in the emission at 600 nm over time (Figure S5). While all the nanostructures showed similar deintercalation kinetics, removal of EBr from the duplex was slightly different compared to that of the nanostructures. This time-dependent change in fluorescence of EBr shows that caffeine dislodges the dye from the duplex as well as the DNA nanostructures. Since the interaction of EBr with caffeine also leads to an increase in its fluorescence at 600 nm,[33] the deintercalation of the dye could not be quantified using fluorescence spectroscopy. We note that the time-dependent change in the emission intensity of duplex-EBr complex was characteristically different from that of 3TT-EBr complex (Figure S5).

We then investigated caffeine-induced deintercalation of EBr from DNA nanostructures using non-denaturing PAGE. We ran duplicates of each of the four DNA structures on non-denaturing gels and stained them using 1.27 μM EBr (in 50 mL water). After staining, we sliced the gels to separate the duplicate lanes, and soaked one duplicate in 1× TAE-Mg^{2+} buffer and the other in 50 mM caffeine in the dark. We imaged the gel slices every 5 min for up to 45 min (Figures 4A and S6). The decrease in the intensity of the band corresponding to the DNA structures was more prominent in caffeine-soaked gels compared to the control soaked in buffer. We also observed a decrease in band intensity in gels soaked in buffer, possibly due to diffusion of the DNA molecules from the porous gel matrix.[34] To quantify deintercalation, we measured the intensity of the bands at different time points and calculated the percent deintercalation in caffeine compared to the samples soaked in buffer [% deintercalation = $(I_{buffer}-I_{caffeine})/I_{buffer}$) x 100]. In all cases, we observed that >90% EBr was removed within 45 min (Figures 4B and S7). While PAGE-based analysis does not provide high time resolution for kinetics studies, we observed that the initial rate of deintercalation was slightly different for 3TT structure (~80% deintercalation in 15 min) compared to the other structures (~80% deintercalation in the first 10 min).

Intercalation of small molecules into DNA is a well-known phenomenon.[31] Beyond their well-known use in staining nucleic acids in gel electrophoresis, intercalating small molecules are also used in supramolecular assembly and DNA nanotechnology. Our work adds to the existing library of functions that small molecules can perform in combination with DNA nanostructures. For example, small molecules that cause deintercalation can be used to remove EBr from DNA which currently requires the use of chromatography techniques[35] or organic solvent extractions.[36] Related to drug loading and delivery, our results show that complex DNA nanostructures can be used not only to carry intercalating drugs but their release profiles can also be potentially tuned using other small molecules (such as caffeine shown here). Further studies on loading of drugs onto various DNA nanostructures and triggered release of the drugs using physiologically relevant small molecules may prove useful for clinical applications.

Limitations of the study

Our work provides new information on the deintercalation of small molecules (with EBr as an example) from DNA nanostructures using caffeine. While our work shows similar deintercalation levels for DNA motifs with

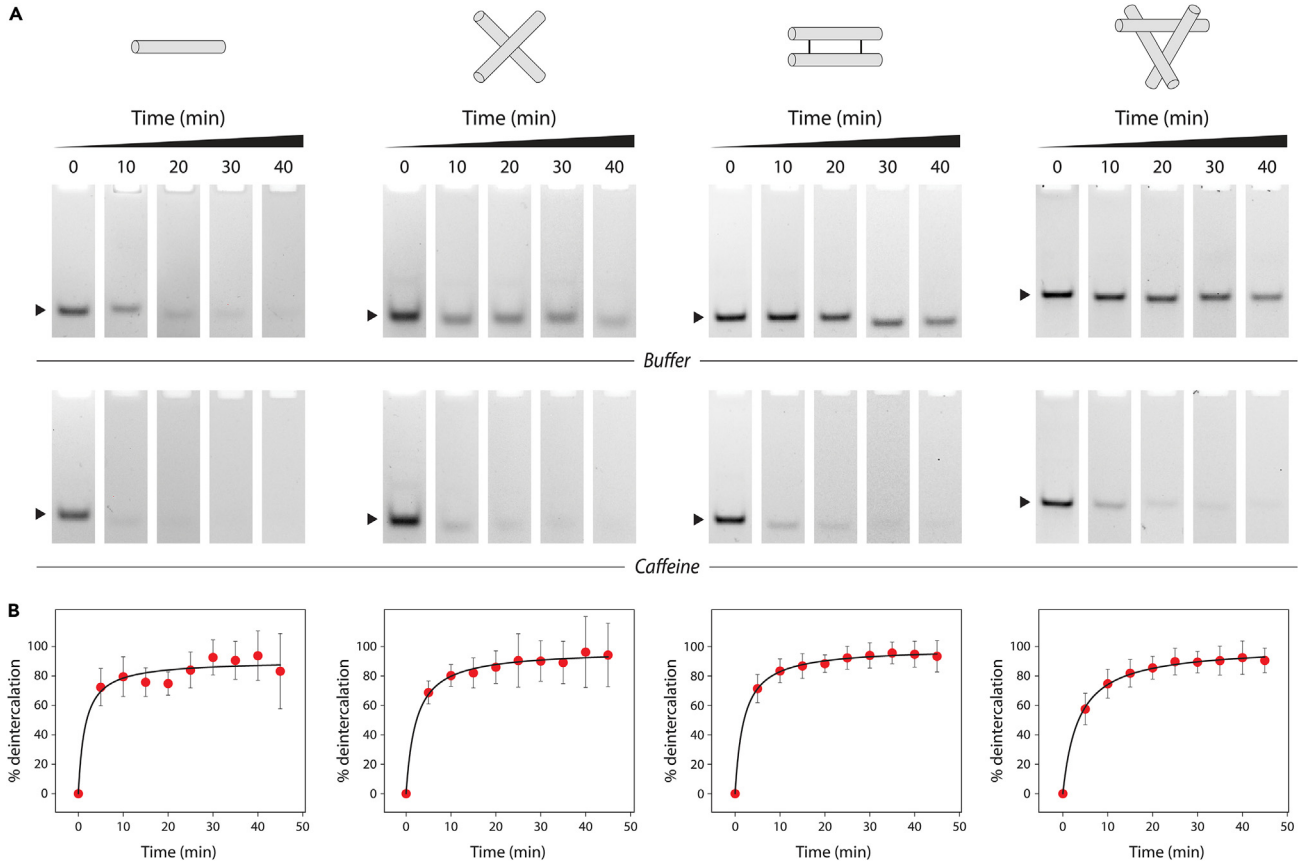

Figure 4. Caffeine-induced deintercalation of ethidium bromide from DNA nanostructures

(A) Non-denaturing gels for different DNA structures stained with ethidium bromide and soaked either in buffer (top row) or caffeine (bottom row).

(B) Percent deintercalation in different DNA nanostructures measured using the decrease in band intensity in buffer and caffeine. Data represent mean and error propagated from standard deviations of triplicate experiments. See Figure S6 for gel images of all time points and Figure S7 for a plot containing data from all four structures overlapped.

multiple crossovers compared to duplex DNA (all structures show >90% deintercalation in 45 min), we also observed slight differences in the deintercalation profiles (Figure S5). More work is needed to attribute any structural effect to this process, such as the effect of crossovers on intercalation and deintercalation. While we suggest that small molecule-induced deintercalation can be useful for triggered release of drugs intercalated in DNA nanocarriers, our work only shows a demonstration of this using the common intercalator EBr, and more work is needed to test this process for other established intercalating drugs.

STAR★METHODS

Detailed methods are provided in the online version of this paper and include the following:

- KEY RESOURCES TABLE
- RESOURCE AVAILABILITY
  - Lead contact
  - Materials availability
  - Data and code availability
- METHOD DETAILS
  - Assembly of DNA complexes
  - Preparation of DNA-EBr complexes
  - Caffeine treatment of DNA-EBr complexes for fluorescence spectroscopy
  - Measurement of fluorescence emission spectra

- Kinetics measurement
- Caffeine treatment of DNA in polyacrylamide gels
- QUANTIFICATION AND STATISTICAL ANALYSIS

SUPPLEMENTAL INFORMATION

Supplemental information can be found online at https://doi.org/10.1016/j.isci.2023.106564.

ACKNOWLEDGMENTS

Research reported in this publication was supported by the University at Albany, State University of New York and The RNA Institute start-up funds to A.R.C.

AUTHOR CONTRIBUTIONS

B.R.M. designed and performed experiments, analyzed and visualized data, and wrote the manuscript. S.C. and C.P. performed experiments. A.R.C. conceived and supervised the project, acquired funding, designed experiments, analyzed and visualized data, and wrote the manuscript.

DECLARATION OF INTERESTS

A.R.C. is a member of the editorial advisory board of iScience.

Received: January 22, 2023
Revised: March 2, 2023
Accepted: March 28, 2023
Published: April 1, 2023

REFERENCES

1. Persil, Ö., and Hud, N.V. (2007). Harnessing DNA intercalation. Trends Biotechnol. *25*, 433–436. https://doi.org/10.1016/j.tibtech.2007.08.003.

2. Chandrasekaran, A.R., MacIsaac, M., Dey, P., Levchenko, O., Zhou, L., Andres, M., Dey, B.K., and Halvorsen, K. (2019). Cellular microRNA detection with miRacles: microRNA- activated conditional looping of engineered switches. Sci. Adv. *5*, eaau9443. https://doi.org/10.1126/sciadv.aau9443.

3. Heck, C., Torchinsky, D., Nifker, G., Gularek, F., Michaeli, Y., Weinhold, E., and Ebenstein, Y. (2020). Label as you fold: methyltransferase-assisted functionalization of DNA nanostructures. Nanoscale *12*, 20287–20291. https://doi.org/10.1039/D0NR03694C.

4. Özhalıcı-Ünal, H., and Armitage, B.A. (2009). Fluorescent DNA nanotags based on a self-assembled DNA tetrahedron. ACS Nano *3*, 425–433. https://doi.org/10.1021/nn800727x.

5. Moradpour Hafshejani, S., Watson, S.M.D., Tuite, E.M., and Pike, A.R. (2015). Click modification of Diazido Acridine intercalators: a versatile route towards Decorated DNA nanostructures. Chemistry *21*, 12611–12615. https://doi.org/10.1002/chem.201501836.

6. Liu, M., Ma, W., Zhao, D., Li, J., Li, Q., Liu, Y., Hao, L., and Lin, Y. (2021). Enhanced penetrability of a tetrahedral framework nucleic acid by modification with iRGD for DOX-targeted delivery to triple-negative breast cancer. ACS Appl. Mater. Interfaces *13*, 25825–25835. https://doi.org/10.1021/acsami.1c07297.

7. Zhang, Q., Jiang, Q., Li, N., Dai, L., Liu, Q., Song, L., Wang, J., Li, Y., Tian, J., Ding, B., et al. (2014). DNA origami as an in vivo drug delivery vehicle for cancer therapy. ACS Nano *8*, 6633–6643. https://doi.org/10.1021/nn502058j.

8. Zhao, Y.-X., Shaw, A., Zeng, X., Benson, E., Nyström, A.M., and Högberg, B. (2012). DNA origami delivery system for cancer therapy with tunable release properties. ACS Nano *6*, 8684–8691. https://doi.org/10.1021/nn3022662.

9. Hu, Q., Li, H., Wang, L., Gu, H., and Fan, C. (2019). DNA nanotechnology-enabled drug delivery systems. Chem. Rev. *119*, 6459–6506. https://doi.org/10.1021/acs.chemrev.7b00663.

10. Madhanagopal, B.R., Zhang, S., Demirel, E., Wady, H., and Chandrasekaran, A.R. (2018). DNA nanocarriers: programmed to deliver. Trends Biochem. Sci. *43*, 997–1013. https://doi.org/10.1016/j.tibs.2018.09.010.

11. Miller, H.L., Contera, S., Wollman, A.J.M., Hirst, A., Dunn, K.E., Schröter, S., O'Connell, D., and Leake, M.C. (2020). Biophysical characterisation of DNA origami nanostructures reveals inaccessibility to intercalation binding sites. Nanotechnology *31*, 235605. https://doi.org/10.1088/1361-6528/ab7a2b.

12. Xu, Y., Huang, S.W., Ma, Y.Q., and Ding, H.M. (2022). Loading of DOX into a tetrahedral DNA nanostructure: the corner does matter. Nanoscale Adv. *4*, 754–760. https://doi.org/10.1039/D1NA00753J.

13. Ijäs, H., Shen, B., Heuer-Jungemann, A., Keller, A., Kostiainen, M.A., Liedl, T., Ihalainen, J.A., and Linko, V. (2021). Unraveling the interaction between doxorubicin and DNA origami nanostructures for customizable chemotherapeutic drug release. Nucleic Acids Res. *49*, 3048–3062. https://doi.org/10.1093/nar/gkab097.

14. Nehlig, A., Daval, J.-L., and Debry, G. (1992). Caffeine and the central nervous system: mechanisms of action, biochemical, metabolic and psychostimulant effects. Brain Res. Rev. *17*, 139–170. https://doi.org/10.1016/0165-0173(92)90012-B.

15. Selby, C.P., and Sancar, A. (1990). Molecular mechanisms of DNA repair inhibition by caffeine. Proc. Natl. Acad. Sci. USA *87*, 3522–3525. https://doi.org/10.1073/pnas.87.9.3522.

16. Fritzsche, H., Lang, H., Sprinz, H., and Pohle, W. (1980). On the interaction of caffeine with nucleic acids: IV. Studies of the caffeine-DNA interaction by infrared and ultraviolet linear dichroism, proton and deuteron nuclear magnetic resonance. Biophys. Chem. *11*, 121–131. https://doi.org/10.1016/0301-4622(80)85014-9.

17. Davies, D.B., Veselkov, D.A., Djimant, L.N., and Veselkov, A.N. (2001). Hetero-association of caffeine and aromatic drugs and their competitive binding with a DNA oligomer. Eur. Biophys. J. *30*, 354–366. https://doi.org/10.1007/s002490100150.

18. Bedner, E., Du, L., Traganos, F., and Darzynkiewicz, Z. (2001). Caffeine dissociates complexes between DNA and intercalating dyes: Application for bleaching fluorochrome-stained cells for their subsequent restaining and analysis by laser scanning cytometry. Cytometry *43*, 38–45. https://doi.org/10.1002/1097-0320(20010101)43:1<38::AID-CYTO1017>3.0.CO;2-S.

19. Traganos, F., Kapuscinski, J., and Darzynkiewicz, Z. (1991). Caffeine modulates the effects of DNA-intercalating drugs in vitro: a flow cytometric and spectrophotometric analysis of caffeine interaction with novantrone, doxorubicin, ellipticine, and the doxorubicin Analogue AD1981. Cancer Res. *51*, 3682–3689.

20. Baranovsky, S.F., Bolotin, P.A., Evstigneev, M.P., and Chernyshev, D.N. (2009). Interaction of ethidium bromide and caffeine with DNA in aqueous solution. J. Appl. Spectrosc. *76*, 132–139. https://doi.org/10.1007/s10812-009-9139-5.

21. Kallenbach, N.R., Ma, R.-I., and Seeman, N.C. (1983). An immobile nucleic acid junction constructed from oligonucleotides. Nature *305*, 829–831. https://doi.org/10.1038/305829a0.

22. Fu, T.J., and Seeman, N.C. (1993). DNA double-crossover molecules. Biochemistry *32*, 3211–3220. https://doi.org/10.1021/bi00064a003.

23. Winfree, E., Liu, F., Wenzler, L.A., and Seeman, N.C. (1998). Design and self-assembly of two-dimensional DNA crystals. Nature *394*, 539–544. https://doi.org/10.1038/28998.

24. Stewart, J.M., Subramanian, H.K.K., and Franco, E. (2017). Self-assembly of multi-stranded RNA motifs into lattices and tubular structures. Nucleic Acids Res. *45*, 5449–5457. https://doi.org/10.1093/nar/gkx063.

25. Liu, D., Wang, M., Deng, Z., Walulu, R., and Mao, C. (2004). Tensegrity: construction of rigid DNA triangles with flexible four-Arm DNA junctions. J. Am. Chem. Soc. *126*, 2324–2325. https://doi.org/10.1021/ja031754r.

26. Zheng, J., Birktoft, J.J., Chen, Y., Wang, T., Sha, R., Constantinou, P.E., Ginell, S.L., Mao, C., and Seeman, N.C. (2009). From molecular to macroscopic via the rational design of a self-assembled 3D DNA crystal. Nature *461*, 74–77. https://doi.org/10.1038/nature08274.

27. Rusling, D.A., Chandrasekaran, A.R., Ohayon, Y.P., Brown, T., Fox, K.R., Sha, R., Mao, C., and Seeman, N.C. (2014). Functionalizing designer DNA crystals with a triple-helical veneer. Angew. Chem. Int. Ed. Engl. *53*, 3979–3982. https://doi.org/10.1002/anie.201309914.

28. Chandrasekaran, A.R., Vilcapoma, J., Dey, P., Wong-Deyrup, S.W., Dey, B.K., and Halvorsen, K. (2020). Exceptional nuclease resistance of paranemic crossover (PX) DNA and crossover-dependent biostability of DNA motifs. J. Am. Chem. Soc. *142*, 6814–6821. https://doi.org/10.1021/jacs.0c02211.

29. Valsangkar, V.A., Chandrasekaran, A.R., Zhuo, L., Mao, S., Lee, G.W., Kizer, M., Wang, X., Halvorsen, K., and Sheng, J. (2019). Click and photo-release dual-functional nucleic acid nanostructures. Chem. Commun. *55*, 9709–9712. https://doi.org/10.1039/C9CC03806J.

30. Chandrasekaran, A.R., Mathivanan, J., Ebrahimi, P., Vilcapoma, J., Chen, A.A., Halvorsen, K., and Sheng, J. (2020). Hybrid DNA/RNA nanostructures with 2′-5′ linkages. Nanoscale *12*, 21583–21590. https://doi.org/10.1039/D0NR05846G.

31. Olmsted, J., 3rd, and Kearns, D.R. (1977). Mechanism of ethidium bromide fluorescence enhancement on binding to nucleic acids. Biochemistry *16*, 3647–3654. https://doi.org/10.1021/bi00635a022.

32. Hayashi, M., and Harada, Y. (2007). Direct observation of the reversible unwinding of a single DNA molecule caused by the intercalation of ethidium bromide. Nucleic Acids Res. *35*, e125. https://doi.org/10.1093/nar/gkm529.

33. Banerjee, S., Bhowmik, D., Verma, P.K., Mitra, R.K., Sidhhanta, A., Basu, G., and Pal, S.K. (2011). Ultrafast spectroscopic study on caffeine mediated dissociation of mutagenic ethidium from synthetic DNA and various cell nuclei. J. Phys. Chem. B *115*, 14776–14783. https://doi.org/10.1021/jp206300x.

34. Pluen, A., Netti, P.A., Jain, R.K., and Berk, D.A. (1999). Diffusion of macromolecules in Agarose gels: comparison of linear and globular configurations. Biophys. J. *77*, 542–552. https://doi.org/10.1016/S0006-3495(99)76911-0.

35. Sambrook, J., and Russell, D.W. (2006). Removal of ethidium bromide from DNA by ion-exchange chromatography. CSH Protoc. *2006*. pdb.prot3915. https://doi.org/10.1101/pdb.prot3915.

36. Sambrook, J., and Russell, D.W. (2006). Removal of ethidium bromide from DNA by extraction with organic solvents. CSH Protoc. *2006*. pdb.prot3914. https://doi.org/10.1101/pdb.prot3914.

STAR★METHODS

KEY RESOURCES TABLE

REAGENT or RESOURCE	SOURCE	IDENTIFIER
Chemicals, peptides, and recombinant proteins		
Ethidium bromide	VWR Life Science	Cat# X328; CAS: 1239-45-8
Caffeine	Thermo Scientific	Cat# 039214.14; CAS: 58-08-2
40% polyacrylamide solution	National Diagnostics	Cat# EC-850
Oligonucleotides		
See Table S1 for a list of all the DNA sequences	Integrated DNA Technologies (IDT)	N/A
Software and algorithms		
Image Lab version 6.1	Bio-Rad	https://www.bio-rad.com/en-us/product/image-lab-software?ID=KRE6P5E8Z
Origin 2019	OriginLab	https://www.originlab.com/2019
Other		
Bio-Rad Gel Doc XR+ imager	Bio-Rad	https://www.bio-rad.com/en-us/product/gel-doc-xr-gel-documentation-system
Envision XCite 2105 Multimode Plate Reader	PerkinElmer	https://www.perkinelmer.com/product/envision-hts-plate-reader-2105-0010

RESOURCE AVAILABILITY

Lead contact

Further information and requests for resources should be directed to and will be fulfilled by the lead contact: Arun Richard Chandrasekaran (arun@albany.edu).

Materials availability

This study did not generate any new reagents.

Data and code availability

- Data reported in this paper will be shared by the lead contact upon request.
- This paper does not report original code.
- Any additional information required to reanalyze the data reported in this paper is available from the lead contact upon request.

METHOD DETAILS

Assembly of DNA complexes

Duplex

DNA strands D1 and D2 were mixed in equimolar ratios in 1× TAE-Mg^{2+} buffer (40 mM tris base (pH 8), 20 mM acetic acid, 2 mM EDTA, and 12.5 mM magnesium acetate) at a final DNA concentration of 10 μM. The mixture was annealed in a T100 Thermal Cycler (Bio-Rad) from 90 °C to 20 °C over a period of 30 min. The concentration of the base pairs in the solution was 210 μM.

Four-way junction (4WJ)

DNA strands 4WJ1, 4WJ2, 4WJ3, and 4WJ4 were mixed in equimolar ratios in 1× TAE-Mg^{2+} buffer at a final concentration of 10 μM. The mixture was annealed in a T100 Thermal Cycler using the following protocol: 90 °C for 5 min, 65 °C for 20 min, 45 °C for 20 min, 37 °C for 30 min, and 20 °C for 30 min. The concentration of the base pairs in the solution was 320 μM.

Double crossover (DX) motif

DNA strands DX1, DX2, DX3, and DX4 were mixed in equimolar ratios in 1× TAE-Mg^{2+} buffer at a final concentration of 10 μM. The mixture was annealed in a T100 Thermal Cycler using the following protocol: 90 °C for 5 min, 65 °C for 20 min, 45 °C for 20 min, 37 °C for 30 min, and 20 °C for 30 min. The concentration of the base pairs in the solution was 760 μM.

3-turn tensegrity triangle (3TT)

DNA strands 3TT1, 3TT2, and 3TT3 were mixed in 3:3:1 ratio in 1× TAE-Mg^{2+} buffer. The final concentrations of the strands were 30 μM, 30 μM, and 10 μM, respectively. The mixture was annealed in a T100 Thermal Cycler using the following protocol: 90 °C for 5 min, 65 °C for 20 min, 45 °C for 20 min, 37 °C for 30 min, and 20 °C for 30 min. The concentration of the base pairs in the solution was 930 μM.

Preparation of DNA-EBr complexes

DNA-EBr complexes were prepared by mixing DNA and EBr in the required concentrations in 1× TAE-Mg^{2+} buffer (pH 8). The final volume of the samples was 50 μl. The solutions were incubated in dark at 20 °C for 30 min before being transferred to a 386-well plate to measure the fluorescence emission spectra.

Caffeine treatment of DNA-EBr complexes for fluorescence spectroscopy

Different concentrations of caffeine were prepared in de-ionized water. EBr-caffeine mixtures with different EBr:caffeine ratios were prepared in 1× TAE-Mg^{2+} buffer (final concentration of EBr was 20 μM and caffeine concentrations ranged from 0.5 mM to 25 mM in the final solution). The solutions were incubated in dark at 20 °C for 30 min and then transferred to a 386-well plate for fluorescence measurement of the EBr-caffeine mixture. To these solutions, duplex, 4WJ, DX, or 3TT solutions were added at a final base pair concentration of 40 μM. The solutions were incubated in dark at 20 °C for 30 min before measuring the emission spectra for the EBr-caffeine/DNA mixtures.

Measurement of fluorescence emission spectra

The samples were taken in a 386-well plate, and the plate was loaded into Envision XCite 2105 Multimode Plate Reader (PerkinElmer) equipped with 360 nm long pass cutoff excitation filter. The solutions were illuminated with 520 nm and the emission spectra was recorded in the range of 540 nm to 720 nm with a resolution of 1 nm, and each measurement was the sum of 500 flashes. The emission intensity at 600 nm of the solution with EBr or EBr-caffeine mixture was considered as intensity I_0, and the emission intensity of the samples with DNA was considered as intensity I. Fluorescence fold change was calculated as $(I-I_0)/I_0$.

Kinetics measurement

DNA-EBr complexes were placed in a 386-well plate and required volumes of aqueous stock solution of caffeine (100 mM) was added and emission at 600 nm was measured at 30 s intervals for a period of 60 min (using the settings described above). The final concentration of DNA, EBr, and caffeine were 120 μM basepairs, 60 μM, and 50 mM, respectively.

Caffeine treatment of DNA in polyacrylamide gels

Non-denaturing polyacrylamide gels (10% for duplex, 8% for 4WJ, and 6% for DX and 3TT) were prepared using 19:1 acrylamide solution (Accugel, National diagnostics) in 1× TAE- Mg^{2+} buffer. 100 pmol of duplex, 4WJ, DX, or 3TT DNA complexes were mixed with 1 μl of 10× loading dye containing bromophenol blue and glycerol and loaded in the gels. Gels were run at 100 V for 60 min at 4 °C. Gels were stained in 50 ml of 1.27 μM ethidium bromide (in water) for 20 min in dark and imaged on a Bio-Rad Gel Doc XR+ imager. Gels containing the duplicate bands of interest were sliced and soaked in either 1× TAE-Mg^{2+} buffer (control) or a solution of caffeine (50 mM) in 1× TAE- Mg^{2+} buffer. Gels were imaged at 5 min intervals, and the intensity of the bands were quantified using ImageLab (Bio-Rad). The measured band intensities were normalized to the maximum intensity at time 0 min.

QUANTIFICATION AND STATISTICAL ANALYSIS

All experiments discussed in the manuscript were performed with three replicates and data are presented as mean and standard deviation. Statistical details of experiments can be found in figure legends where applicable.